THE INTERNAL SCATTERING OF ULTRASOUND BY BIOLOGICAL TISSUES

by

ANN B. MANSFIELD

Submitted in Partial Fulfillment
of the Requirements for the
Degree of Bachelor of Science
at the
MASSACHUSETTS INSTITUTE OF TECHNOLOGY
June, 1976

Signature redacted

Signature of Author.....
Department of Mechanical Engineering, May 7, 1976

Signature redacted

Certified by.....
Thesis Supervisor

Signature redacted

Accepted by.....
Chairperson, Departmental Committee on Theses

THE INTERNAL SCATTERING OF ULTRASOUND BY BIOLOGICAL TISSUES

by

ANN B. MANSFIELD

Submitted to the Department of Mechanical Engineering on May 7, 1976 in partial fulfillment of the requirements for the Degree of Bachelor of Science.

ABSTRACT

The patterns of signal amplitude vs. angular position which result when diagnostic-level ultrasound is internally scattered by various biological tissues have been studied. The physical phenomenon is similar to Bragg diffraction, which is seen if a wavefront impinges upon a regular array of scattering surfaces whose spacing is of the same order as the incident wavelength, and whose size is smaller than that of the incident wavelength. The internal geometry of the target and the ultrasonic frequency determine a series of maxima and minima occurring with a specific angular pattern in accordance with the Bragg $\sin\theta = n\lambda/2d$ dependence.

Two matched, unfocused ultrasonic transducers, operating as a transmitter and a receiver were excited in a continuous-wave burst mode. The burst duration was long enough (20 μsec) for a continuous-wave approximation to be made, but short enough to be spaced away in time from the large specimen tank reflections. The signals from the receiving transducer were time-gated, rectified, and integrated to obtain an average amplitude, which was plotted as a function of transducer angle. These scans were performed for many frequencies.

Control targets whose geometry was precisely known, and various tissue samples, including pig liver, calf liver, calf muscle, and calf heart, were investigated. Each produced a characteristic scattering profile as well as an identifiable frequency dependence. The tissue structure can be correlated to the calculated array distance present in the Bragg formula. Internal scattering appears to hold diagnostic promise in characterizing abnormal tissue structures by measuring the resulting changes in their interference patterns.

Thesis Supervisor: Padmakar P. Lele
Title: Professor of Experimental Medicine

ACKNOWLEDGEMENTS

The success of this thesis could not have been possible without the help and assistance of many friends and colleagues who contributed their talents. Dr. Padmaker P. Lele was a source of advice and encouragement throughout the entire research project. Dr. Nagabhusan Senapati was also a great aid in the progress of this thesis; he was always available for consultation, and his experience in ultrasonic scattering proved to be invaluable.

The experimental work itself could never have proceeded as smoothly and painlessly as it did with the practical suggestions and cooperation of my fellow students and the staff of the Laboratory for Medical Ultrasonics. I wish to thank Ron Frere, Martin Mason, Robert Martin, Jeffrey Stein, John Csuri, and Alma Murphy. Mr. Kenneth E. Greene, Jr. was always available for help in laboratory techniques, and I thank him for the beautifully-done histology slides which he made for this research project.

Grateful appreciation and thanks are given to my fiance, Andrew Hawryluk, whose patience and understanding helped me through many exasperating weeks of work on this thesis.

This work was supported in part by the U.S. Public Health Service, through grants FD-00680 and GM-19706.

TABLE OF CONTENTS

LIST OF FIGURES

CHAPTER I

INTRODUCTION

A. Ultrasound as a Diagnostic Aid

Medical ultrasonic techniques are usually based on the propagation of high frequency (Megahertz range) longitudinal waves of sound, generated by a piezoelectric transducer connected to a Radio-frequency oscillator. The transducer converts the electrical input to local variations of pressure which propagate through the media in which the transducer is placed.

The diagnostic value of ultrasound has long been recognized as a powerful aid in the visualization of soft tissue structures which are inaccessible by most other noninvasive methods. The traditional applications of ultrasound are based upon the reflection of acoustic pulses at interfaces of varying characteristic impedence. For example, A-scope presents echo amplitude as a function of distance, B-scan presents a cross-sectional view of the reflecting surfaces, and Doppler techniques measure velocity on the basis of the frequency shifts of the reflected wavefront relative to the incident wavefront. A survey of such techniques may be found in Wells (1969).[1]

Only more recently have diagnostic and medical applications based on other tissue parameters and tissue interactions with ultrasound become fields of research. The absorption coefficient appears to be a sensitive indicator of tissue physiological state (Dunn, Edmonds, Fry, 1969).[2] More recently, tissue attenuation was shown to be an accurate indicator of tissue

state (Namery, 1973).[3]

Very little research has been aimed at tissue characterization on the basis of its scattering interactions with ultrasound. Scattering had been considered a nuisance which blurred the images obtained in echo techniques, especially B-scan, but not a useful diagnostic parameter.

B. Experimental Purpose

If changes in scattering characteristics could be correlated with specific tissue physiologies and pathologies, this could become a valuable diagnostic aid. Preliminary to *in vivo* studies, tissue samples were examined *in vitro* to determine the feasibility of detecting tissue structure differences on the basis of the internal scattering properties of the various tissue samples investigated. The samples chosen exhibited great structural differences which could cause a variation of scattering patterns, each characteristic for the tissue under study. If these rather gross differences could be detected, it may prove possible to investigate the smaller differences in scattering which occur in certain pathological states, and correlate the specific disease processes to the diagnostic scattering test results.

The prediction that differences in scattering will be apparent for different tissues, both normal and pathological, is based upon a physical theory of scattering and diffraction of waves which has been used to great advantage in x-ray

crystallography. Wavefronts impinging upon a regular array of small reflecting surfaces produce interference patterns which depend quite specifically upon the physical parameters, such as the spacing of the array.

CHAPTER II

THEORIES OF SCATTERING

A. Surface and Internal Scattering

If one were to consider the specular reflection from an interface with a certain degree of "roughness," surface scattering may occur. If the incident wavelength is small when compared to the characteristic distance between peaks on the rough surface, the reflection becomes non-specular, and the scattering effects increase. The specular reflection amplitude, which is maximum at 90 degrees to the interface plane, is decreased as the wavelength becomes small enough that surface scattering is an important phenomenon. Thus, information about the tissue surface characteristics is contained in the relationship of amplitude to frequency, as well as in the measurement of scattered-signal amplitude at angles other than directly perpendicular to the interface.[4]

Thus, a plane wave incident on a rough surface between two media of differing characteristic impedences appears as a specular reflection with an additional scattered field. If the obstacle in the ultrasonic beam has dimensions which are smaller than, or comparable with the wavelength of the ultrasound, Rayleigh diffraction occurs and the waves change their direction. The amplitude of these scattered waves varies inversely as the square of the incident wavelength. The intensity of the wave which returns toward the source varies inversely as the fourth power of the wavelength.[5,6]

Similar scattering effects can be seen from the internal structural components of tissues as well as from the surface characteristics. Internal structure can be determined by relating the incident wavelength to the spacing of the internal elements which differ slightly in acoustic impedence from the medium surrounding them. For example, x-rays have been employed to investigate the structure of both crystalline and amorphous media by observing the interference effects. Beam components are selectively reinforced or cancelled according to the relative spacing and orientation of scatterers in the beam.

Ultrasound may be used to determine the acoustical structure of tissue, on a scale corresponding to the wavelengths employed, in a completely analogous fashion to x-ray crystallography.[7] The underlying concept is the relation between the spacing of tissue elements, the ultrasonic wavelength, and the scattered signal. There is a selective reinforcement of certain frequencies, such that the Bragg scattering condition:

$$n\lambda = 2d\sin\theta$$

is met. Integral multiples of the wavelength are required for constructive interference to occur.

λ = ultrasonic wavelength

n = integer

d = distance between adjacent scatterers

θ = angle from the horizontal to the scattered signal.

The formula is derived by considering path length differences such that the scattered waves are exactly in phase, yielding maximum constructive interference.[8] This relationship is illustrated in Figure 1.

The tissue may be characterized by either fixing the frequency (and hence λ), and then varying the angle, or by fixing the angle θ and sweeping the frequency so that path length differences vary over a number of wavelengths. Either technique should theoretically yield a succession of signal amplitude peaks, whose spacing is indicative of the target's internal structure.

If one considers a perfect lattice in which the acoustical variations are a series of uniformly spaced impedence discontinuities, the scattered wave will be a periodic series of maxima as either the incident angle or the frequency is changed; each maxima corresponds to a path length difference of an integral number of wavelengths. With this single uniform reflector spacing, a sinusoidal variation of signal amplitude occurs. The Fourier transform of this yields a single peak, whose location is a measure of reflector spacing (d), and whose amplitude is a measure of n (the scatter number).

In biological tissue, changes in acoustic impedence are expected to occur far more randomly than this idealized case. In any particular tissue, the spacings between scatterers may vary widely, but still fall within certain limits that can be statistically specified by the scattering profile shape. In

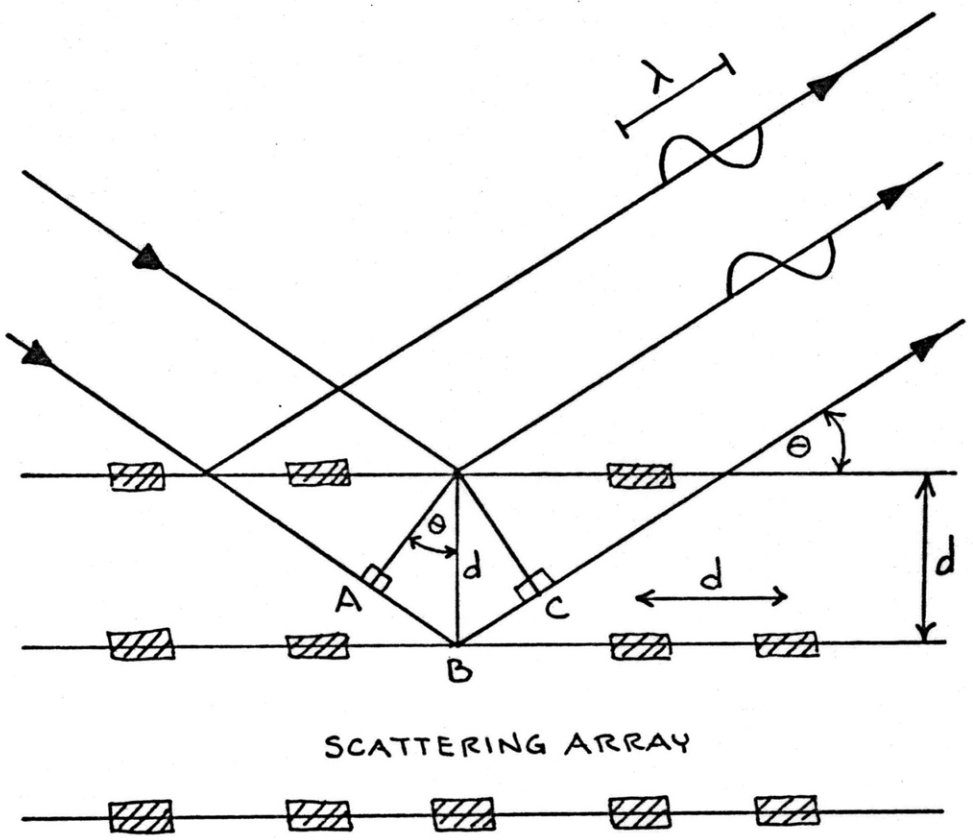

ABC = PATH LENGTH DIFFERENCE = $d\sin\theta + d\sin\theta$

FOR CONSTRUCTIVE INTERFERENCE:

$$2d\sin\theta = n\lambda$$

FIGURE 1: THE GEOMETRY OF BRAGG DIFFRACTION

disease processes, when the structure is altered, the statistical values of d obtained from the scattering profile should also be altered correspondingly.

The effects of randomness introduced into a regular pattern are well-described in x-ray crystallography, which operates on the same Bragg diffraction principle. An "imperfect" lattice structure produces diffracted radiation which is not well-localized. There are strong peaks corresponding to the average ideal lattice, but in other directions the wavelets reflected by the individual scatterers do not cancel perfectly by interference. The peaks are broadened, and weaker diffuse scattering is seen in many directions not specified by the Bragg formula. Thus, there is a corresponding decrease in the intensity of the selective peaks specified by the Bragg law.[9] This is, in general, the type of scattering expected from structures such as seen in highly-organized tissues and organs, where there exists a structural order which is marked by small perturbations, and statistical fluctuations of inter-scatterer distance occur around a certain mean value.

B. Review of Current Research in Ultrasonic Scattering Phenomena

The usefulness of Rayleigh scattering as a measure of tissue surface characteristics was demonstrated by Senapati, Lele, and Woodin in 1972.[10] Surface scattering differed greatly in studies of normal frog liver and necrotic liver due to red-leg disease. The diseased liver showed a broadening of the

scatter profile, probably caused by surface pitting effects and the increased inhomogeneity of the tissue due to random fibrous structures, and the frequent hematomas present. Mountford and Wells[11] also found changes in the reflected signal from the surface of normal and cirrhotic liver, using A-scope technology, and performing a quantitative analysis upon the resulting echoes. Freese and Makow[12] have also observed that the condition of animal tissue greatly effects its backscattering properties. Assuming that the propagation velocity is constant in the tissue under study, the frequencies observed in the A-scope echo train can be directly related to the spatial frequencies of the three-dimensional array of scattering centers that produce it. However, the shape of the pulse and the type of transducer can also affect this scattered spectrum.[13]

Chivers, Hill, and Nicholas[14] investigated several tissue samples <u>in vitro</u>, examining the frequency components of the surface echo. The signal was gated, put through a spectrum analyzer, and the results were displayed as spectral profiles of amplitude vs. frequency. Spectra from various types of tissues appeared strikingly characteristic, differing in amplitude as well as in frequency content. Chivers, Hill, and Nicholas proposed that the distinction might be made merely on the basis of the area under the spectral envelope, and the number of peaks seen. They were also able to demonstrate a dependence of the profile shape upon tissue orientation, thus revealing effects of tissue anisotropy.

C. R. Hill[15] was one of the first to look at the phenomenon of internal tissue scattering, making an "ultrasonic Bragg Diffraction record" of an excised sample with a pulse-echo probe transducer. The angular dependence of amplitude was determined for muscle, spleen, brain, and liver. The scans appeared to reflect the existence of characteristic structural patterns of acoustically reflecting targets within each tissue, which may be related to histological appearance.

Chivers and Hill have also examined internal Bragg scattering by an A-scope echo method in which the transducer position is fixed and the backscattered echo is frequency analyzed. A time-gate was used to monitor specific tissue volumes of interest within the sample, thus localizing internal, as opposed to surface scattering phenomena. The effects of the time-gate were studied; a relationship between the obtained signal and the gate length indicated the inhomogenity of the structure, and the different scatter profiles for adjacent volumes of tissue. Thus, there is a type of averaging process occurring in the time-gate, as well as in space, because of the finite transducer beam width. This is not disadvantageous, since the signals must be treated on a statistical basis. The results of Chivers' and Hill's study indicated that spectral differences could differentiate human and porcine liver on the basis of peak placement, as well as displaying characteristic patterns for fat and spleen, which show more high frequency components.[16]

Recent work in internal scattering as a measure of tissue structure utilized a newer approach to fitting experimental observations to the Bragg formula in hopes of correlating scatter with tissue physiology and pathology. Waag, Gramiak, and Lerner[17] utilized a frequency-sweep technique in which a receiving and transmitting transducer are held at a fixed angular position, and the radio frequency input is swept over a broad range. Controls done with regular periodic reflectors representing abrupt impedence discontinuities yielded well-known Bragg diffraction results, as did plates of varying thicknesses. The geometry of these targets could be easily reconstructed from their amplitude vs. frequency profiles. The prediction that random structures should scatter with the maximum intensity at a frequency inversely related to their size was also shown experimentally. Waag, Gramiak, and Lerner measured the frequency dependence of scattering from normal left ventricular beef heart and heart muscle in which a lesion had been ultrasonically induced. The results show considerable difference; the distribution in the irradiated tissue was more uniform and more high frequency components were contained.

C. Summary

It appears that scattering and diffraction-based probing techniques can be used successfully to characterize the acoustical variations in tissue for medical diagnosis. It is not yet possible to know how much information about a tissue sample may

be obtained in this manner. The variation of density and acoustic impedence across one cell or groups of cells is not yet clear, making it impossible to appreciate the size of biological structures that will be acoustically significant, considering the wavelengths involved.

The internal scattering signals which have been observed in the experiments cited appear to originate from tissues with a complex array of scattering centers. The phenomenon is completely analogous to x-ray diffraction by crystals, and implies that, acoustically, soft tissues behave as a semi-ordered three dimensional array, in which the exact geometry may prove to be characteristic of the particular tissue and the tissue state.

CHAPTER III

EXPERIMENTAL APPARATUS AND PROCEDURE

A. Introduction

There are two general methods of characterizing the internal scattering properties of biological tissues: angle-sweep scanning techniques, such as used by C. R. Hill,[18] or frequency-sweep techniques, such as employed by Waag, Gramiak, and Lerner.[19] In either approach, a tissue sample is placed in a tank of degassed physiological saline, which insures constant acoustic properties of the medium, and two ultrasonic transducers serve as a receiver and a transmitter.

In my experimental work, I chose to study the effects of changing angular position upon the scattered signals, keeping frequency fixed. These scans were then repeated at several discrete frequencies to determine the dependence upon wavelength, and the correlation to the tissue under study.

B. Specimen Tank Design

Several factors were important in designing and building the specimen tank. To facilitate performing angle-sweep scanning, the tank was built to be cylindrical in shape, with two rotating arms to hold the transmitting and receiving transducers. These arms were constructed so that when the transducers were clamped on, they pointed to the precise center of the tank, inside the volume to be occupied by the tissue specimen. The tank could rotate independently of the two transducer arms, as

well, providing for any specimen rotations.

The material chosen was plexiglass, which has a very large acoustic impedence mismatch with the aqueous medium contained by the tank. The result of this would be large reflected echoes which could completely mask the sought-after scattering signal; therefore, a method of making the tank more anechoic was devised. The bottom was covered with an absorber of soft polyethylene, cut with deep, narrow triangular ridges to act as wave-traps. The inside walls were covered with a thin layer of flexible soft polyethylene to aid in both ultrasonic absorption and to reduce the water/plexiglass impedence mismatch. The film of polyethylene served as well as a means of coupling the transducers to the water medium.

Several long, narrow windows were cut into the sides of the plexiglass cylinder, enabling the small transducers to slide in and come in contact with the polyethylene film. A better acoustic coupling was achieved through the use of commercially-available electrode gel. A diagram of the entire tank apparatus is shown in Figure 2.

Specimen size and shape was another factor in the experimental setup. The scattered signals are small, so a minimum path length in the tissue is desirable; however, a larger distance traversed by the transmitted ultrasonic wave is advantageous for gating purposes, to separate the surface signal from the internally scattered echoes. The tissue specimens used were cylindrical plugs of 3 cm diameter, and of a height at least

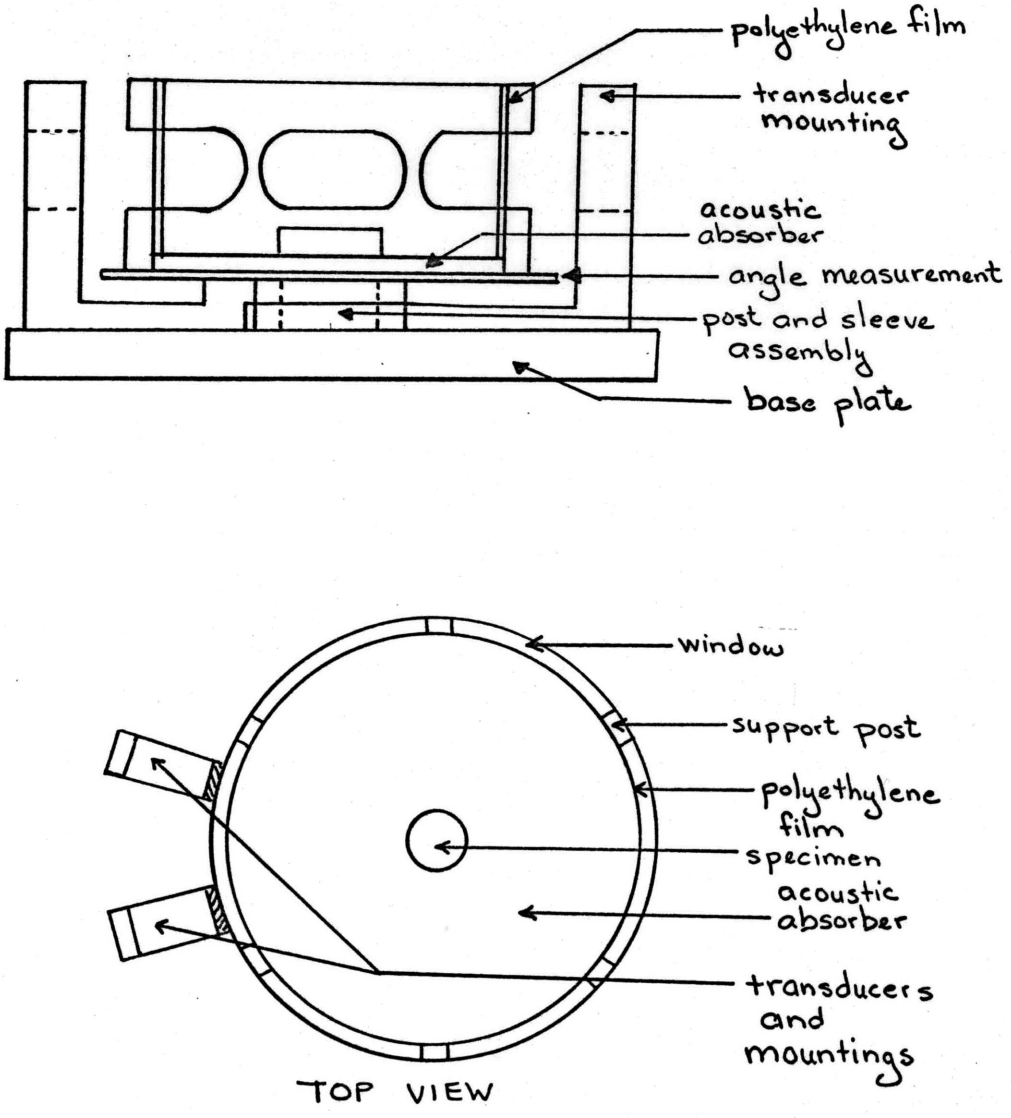

FIGURE 2: SPECIMEN TANK DESIGN (SIDE AND TOP VIEWS)

equal to the diameter of the transducers (approx. 1 cm).

C. Ultrasonic Transducers and Measurement Instrumentation

Two matched, unfocused transducers were used in a continuous-wave burst mode. The pulse duration was sufficiently long, 20 μsec, for a continuous wave approximation to be valid, but short enough to be spaced away temporally from the larger reflections due to the walls of the specimen tank. Several pairs of such matched, diagnostic power level transducers were used to span a range of transmitter frequencies extending from 1 MHz to 4 MHz. Because of the small diameter of the transducers used, the scattering measurements were made in the near field, or Fresnel zone, of the ultrasonic field. In this near-field region, most of the energy is confined to a cylinder with the same diameter as the transducer; however, a non-uniform axial distribution of intensity occurs in this zone of the ultrasonic field. In the far-field, the Fraunhofer zone, the beam begins to diverge, and the axial intensity profile becomes more uniform. The transition from one region to another is given by:[20]

$$x = \frac{4r^2 - \lambda^2}{4\lambda}$$

where: x = distance from transducer to end of near field

r = transducer radius

λ = ultrasonic wavelength.

For the geometry of the ultrasonic field, see Figure 3. The

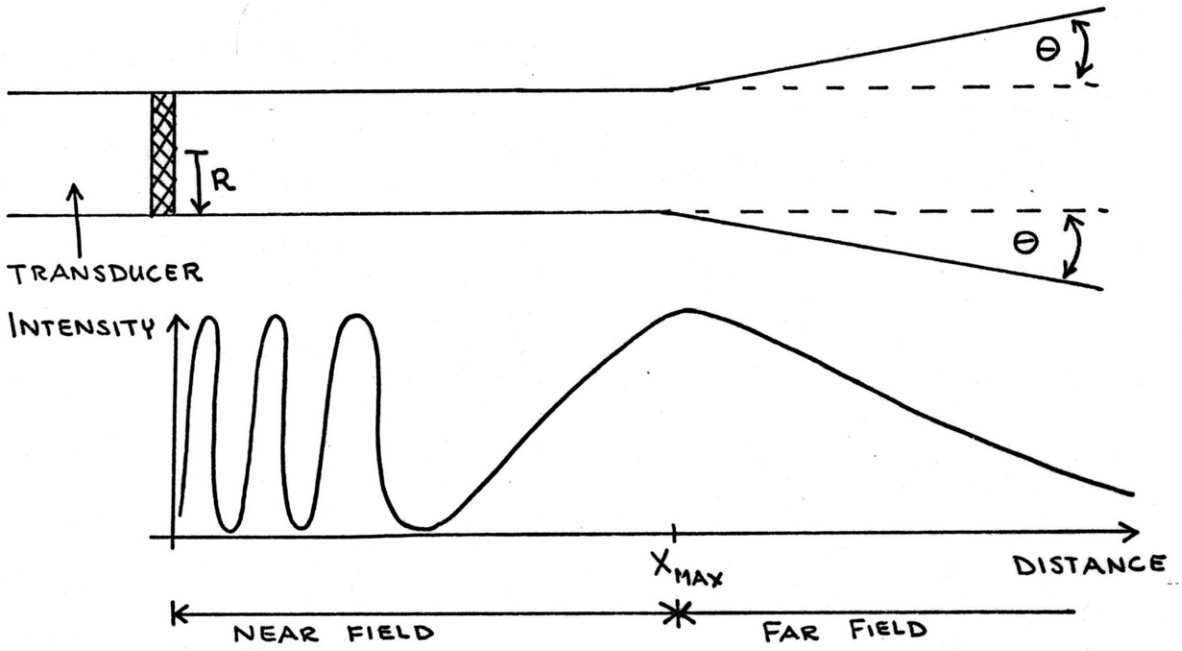

FIGURE 3: THE ULTRASONIC FIELD OF A TRANSDUCER

near field has the further disadvantage that the axial intensity profile has many lobes. However, at the distances involved in this experiment, only the main lobe is of significant intensity. At 2.25 MHZ, with a transducer diameter of 1.5 cm, and a tank radius of 7 cm, the positioning and intensity of the lobes can be determined:

Main lobe - relative intensity = 100%
- divergence angle = 3°
- diameter = 10.74 mm

Second lobes - relative intensity = 17.2%
- divergence angle = 5.6°
- diameter = 19.66 mm

Third lobes - relative intensity = 4.1%
- divergence angle = 8.2°
- diameter = 28.5 mm.

These calculations are based on the formula:[21]

$$\sin\theta = \frac{J_o \lambda}{2\pi r}$$

where: J_o is a Bessel Function

r = transducer radius

λ = ultrasonic wavelength

θ = angular beam divergence
(location of minima on either side of lobe).

A tradeoff exists, therefore, between the ideal intensity distribution, and the need for a small beam width and narrow

divergence to increase the anuglar resolution of the experimental measurements. With the small transducer radius and the operating frequency range used (low enough so that tissue attenuation does not reduce the scattered signal to an immeasurably low level), the length of the near-field region makes building a specimen tank such that the tissue is in the far-field zone impractical. A tank radius of a few feet is necessary for this conditions to be met, as opposed to the 6 inch tank radius employed.

The transmitting transducer was excited in a continuous-wave burst mode by a radio frequency oscillator, which was time-gated by a square wave generator. The frequency, amplitude, and duration of the burst were all independently variable. The scattered signal from the receiving transducer was amplified, and the noise level was reduced by a tuneable bandpass filter adjusted to minimize signals whose frequency was not matched to the ultrasonic frequency. The signal was then rectified, and the resulting envelope was time-gated to eliminate the tank echoes and the echoes from the front and back surfaces of the tissue sample. The time-gated internal scattering signal was integrated by an operational amplifier, and displayed on an oscilloscope. The value of the integrated signal, which assuming constant gating time is proportional to the average amplitude of the internal scattering signal, was recorded as a function of transducer angle. This averaging process, as well as the averaging due to the finite width of the ultrasonic bean, served

to compensate for the intensity variations of the near-field, as well as for the local inhomogeneity of the tissue. Diagnostically, an average measure of the tissue scattering would prove to be more useful than a highly localized determination of scattering profile, considering the variability between various normal tissues from different organisms, and the local variability that exists from one small region of a tissue to another region of the same tissue. A schematic of the experimental apparatus is shown in Figure 4.

D. Angle-Scanning Procedure

Two different scanning procedures were used in the course of this experiment. The first method tried, which can be called an arc-scan, involved holding one transducer fixed and moving the other in a large arc around the tank. Many problems were encountered in this approach, most importantly the detection of the unmodified transmitting beam by the receiving transducer, masking out the much smaller scattered signal. This procedure failed to give very reproducible results, and the profile of amplitude vs. angle was very random and erratic, with very large amplitude fluctuations for small angular changes.

If one considers the physics of Bragg scattering, the reason for the failure of arc-scanning becomes explicable. As shown in Figure 5, there are various planes of scattering elements which can serve as the basic "reflecting surface." Each of these has a different value of d (distance between

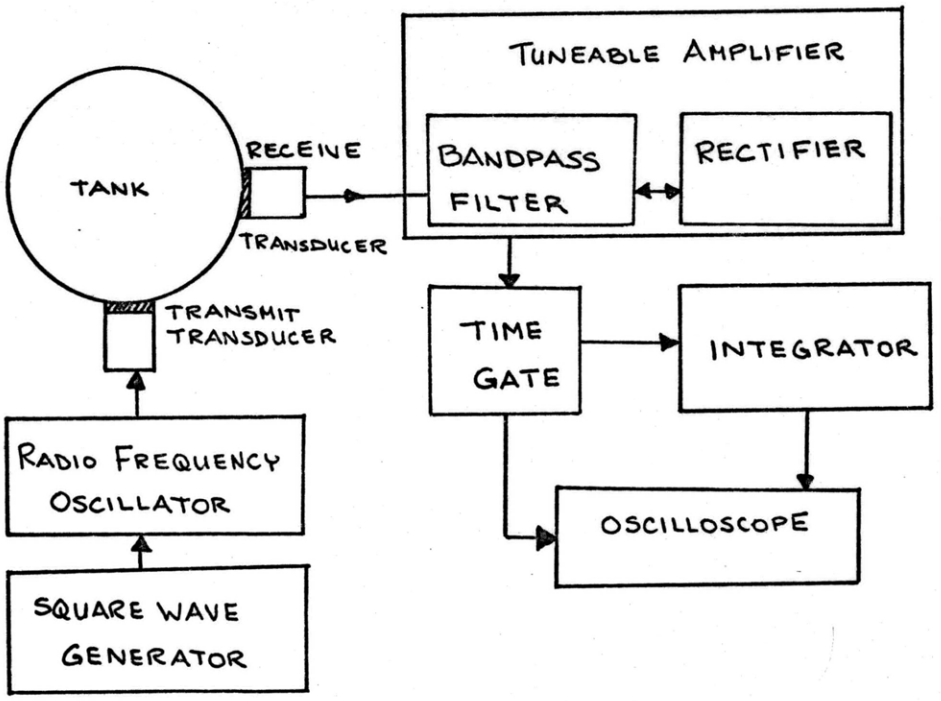

FIGURE 4: SCHEMATIC OF THE EXPERIMENTAL APPARATUS

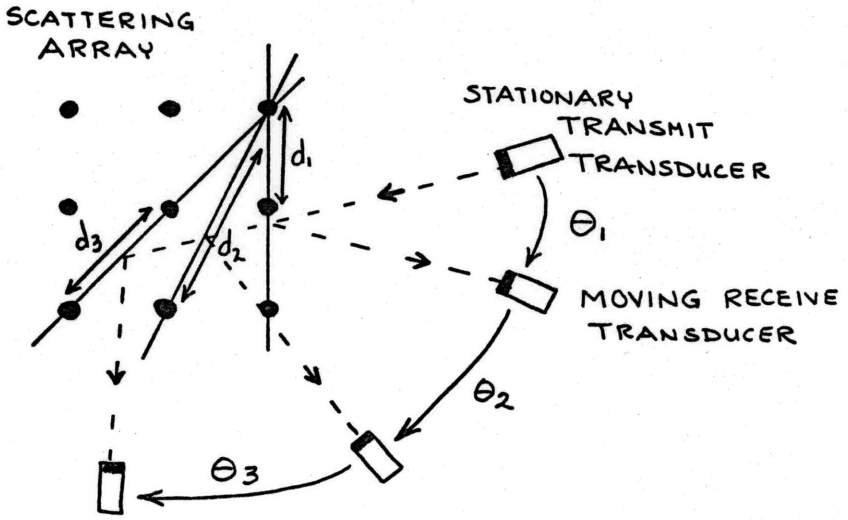

FIGURE 5: ARC-SCANNING AND THE BRAGG FORMULA

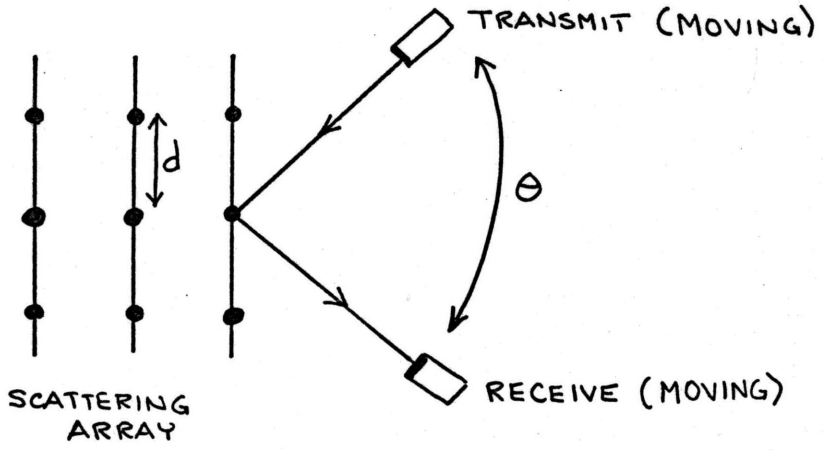

FIGURE 6: DOUBLE-ANGLE SCANNING METHOD

adjacent array elements), and therefore a different requirement for fulfillment of the Bragg condition.

The second method of conducting the angle-sweep scan is by moving both the transmitting and receiving transducers, each an equal amount. Thus, the line of scatterers off which the reflection and interference phenomenon is occurring will be the same for the entire scan, and there should be some values of θ for which the Bragg condition is met. This "double-angle scan" method is illustrated in Figure 6.

Several double-angle scans were done to characterize various tissue specimens, and the results were plotted as amplitude vs. total transducer angle (2θ in the Bragg Law). These scans were repeated at various frequencies to assess the affect of wavelength upon the internal scattering profile.

CHAPTER IV

EXPERIMENTAL RESULTS

A. Results Obtained from Phantom Targets of Known Geometry

To test the feasibility of making these internal scattering measurements, the strength of the signals involved, and the correlation of the results with Bragg diffraction theory, phantom scattering targets of precisely known geometry were used. A scatterer was made of steel pins (diameter 0.026 in.) spaced in a square grid with a distance of 0.10 inches between adjacent pins. Using an ultrasonic frequency of 2.25 MHz, and substituting into the Bragg formula, maxima can be expected to occur at approximately 15°, 30°, 45°, 62°, 81°, 102°, and 131° total transducer angle (2θ). These predictions correlate very well with the experimental result obtained by double-angle scan, shown in Figure 7. The values obtained were highly reproducible, with most of the fluctuations being accountable on the basis of uncertainty in positioning the two transducers. The values plotted are the mean of 5 separate runs, and the relative range of values obtained was approximately 7% of the total signal amplitude. The scattered signals obtained were very strong due to the large acoustic impedence mismatch between the steel pins and the water surrounding them.

In order to better simulate biological tissue's gross acoustic properties, a second phantom target was made of soft polyethylene with holes drilled through it in a regular array. The water-filled holes were 0.026 inches in diameter, and the

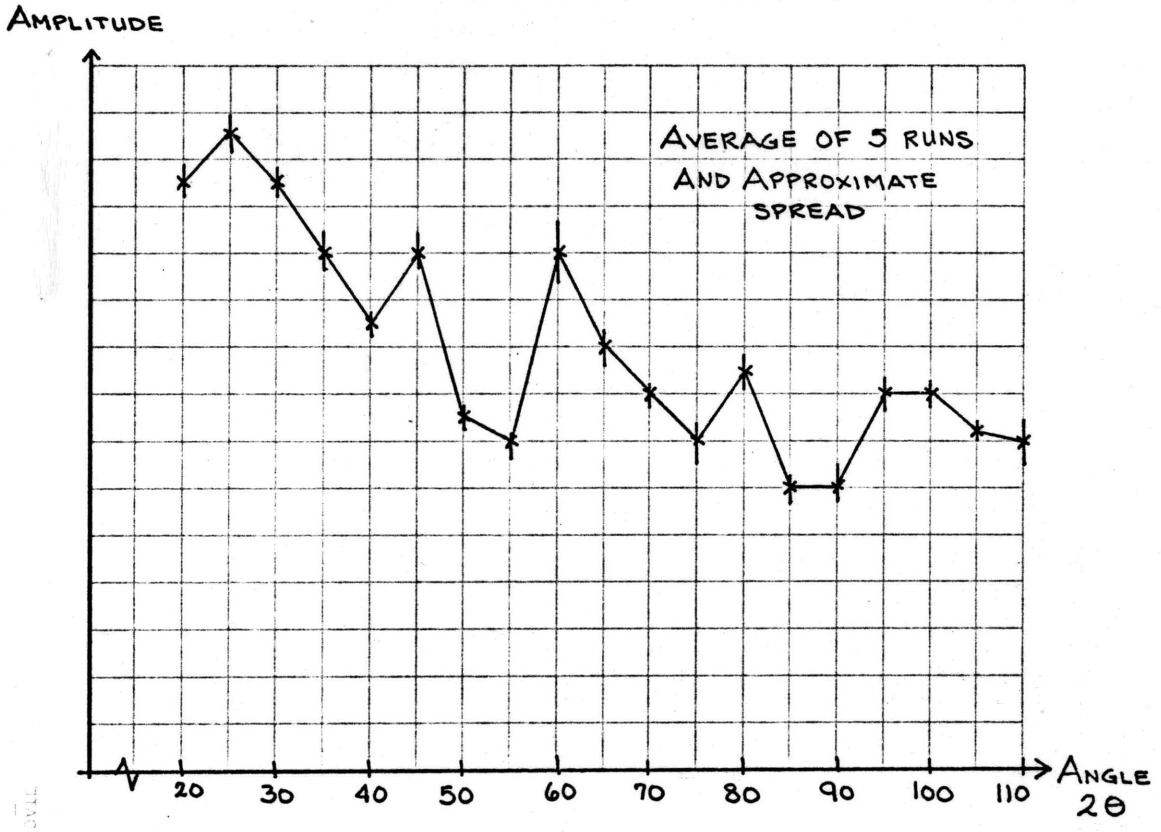

FIGURE 7: SCATTERING PROFILE OF PIN-SCATTERER PHANTOM TARGET

Frequency equals 2.25 Megahertz.

spacing between them was 0.05 inches. According to Bragg's Law, the angular locations of expected maxima are approximately 35° and 70° of total transducer angle, if these measurements are taken at a frequency of 2.25 MHz. The experimental results correlated very well with the theory, and were very reproducible, as seen in Figure 8. The points plotted are the mean values of 5 experimental runs, and the average range of values was approximately 8% of the total signal amplitude. The magnitude of the scattered signal was significantly reduced from the values obtained with the pin-scatterer phantom, due to the fairly small acoustic impedence difference at the water/polyethylene interface, as well as the increased absorption of ultrasonic energy by the polyethylene. In both of these respects, the polyethylene dummy appeared to be a good model of an idealized tissue sample. As a final control run, a cylindrical plug of soft polyethylene without any holes drilled into it was used as the target. The oscillograph trace recorded an echo from the front and back surfaces, but no evidence of any scattering signal from the interior was found, even at very high gain. This indicated that inhomogeneity is indeed the source of the internal scattered echoes, and the phenomenon which we wish to investigate directly caused the signals which we were measuring.

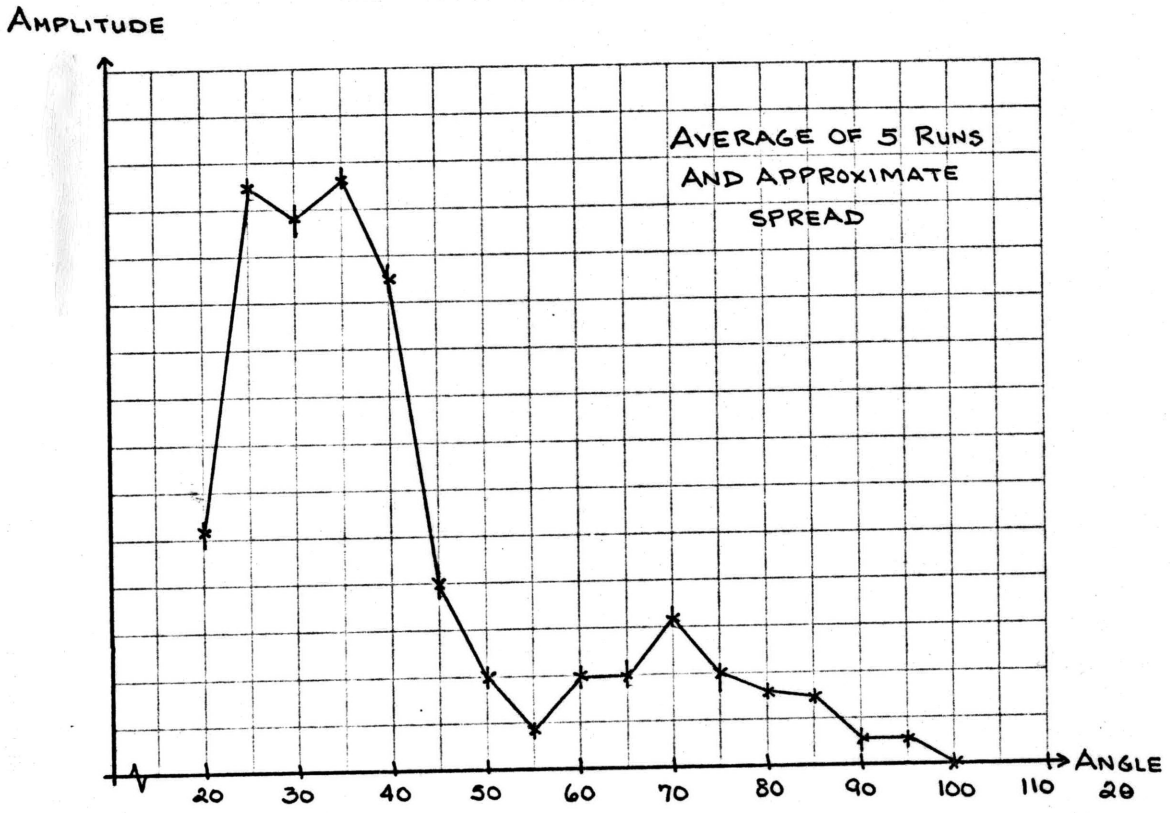

FIGURE 8: SCATTERING PROFILE OF POLYETHYLENE PHANTOM TARGET

Frequency equals 2.25 Megahertz.

B. Results Obtained From Various Biological Tissue Samples

Double-angle scans were performed with many different samples of mammalian tissue from various organs and from various species. Samples of calf liver, pig liver, calf skeletal muscle, and calf cardiac muscle were investigated to determine their characteristic internal scattering profiles. The most striking result is the periodicity of maxima and minima which are evident in the angular dependence of scattered amplitude. The precise values of the signal strength appear not to be important, and were noted to change as the tissue was rotated. However, the average periodicity, the angular distance by which maxima are separated, remained constant for a given tissue at a given incident frequency. For example, at 2.25 MHz, calf liver produced a scattering profile with an average angular separation of approximately 20° of arc. There was a fairly large spread of values for the average periodicity of the scatter profiles, largely due to biological variations from one tissue sample to another. However, when statistical analysis was done on the data, the range of periodicity values evident in calf liver could be demonstrated to be a separate population from the values obtained from other tissue samples, by using the t-test, calculated at the 5% significance level. The value of t is calculated:[22]

$$t = \frac{\bar{x}_1 - \bar{x}_2}{\sqrt{\frac{s_1^2}{N_1} + \frac{s_2^2}{N_2}}}$$

where: $\bar{x}$ = mean

s = standard deviation

N = degrees of freedom

subscripts indicate the two populations. The calculated t value was compared to tabulated values of t at the desired level of significance and the proper number of degrees of freedom. If the calculated value is larger than the tabulated value, the difference is significant.

The important parameter to consider in analyzing the scattering profiles appears to be the average periodicity, and not the relative heights of the maxima. This is evident in Figures 9 and 10, two characteristic scans obtained from calf liver tissue. Although the profiles may appear to be different due to the sample orientation change, the average angular separation of maxima remains constant.

These double-angle scans were performed on many other different tissue samples, each yielding a characteristic scattering profile with a certain average intermaximal separation at the operating frequency of 2.25 MHz. Although these average periodicities were statistically recognizable as several significantly different populations, it was often difficult to tell by eye which type of tissue sample was under study, given the resulting scattering profile. A more reliable method of discriminating tissue type based upon internal scattering properties utilized the frequency dependence of the angular profile patterns.

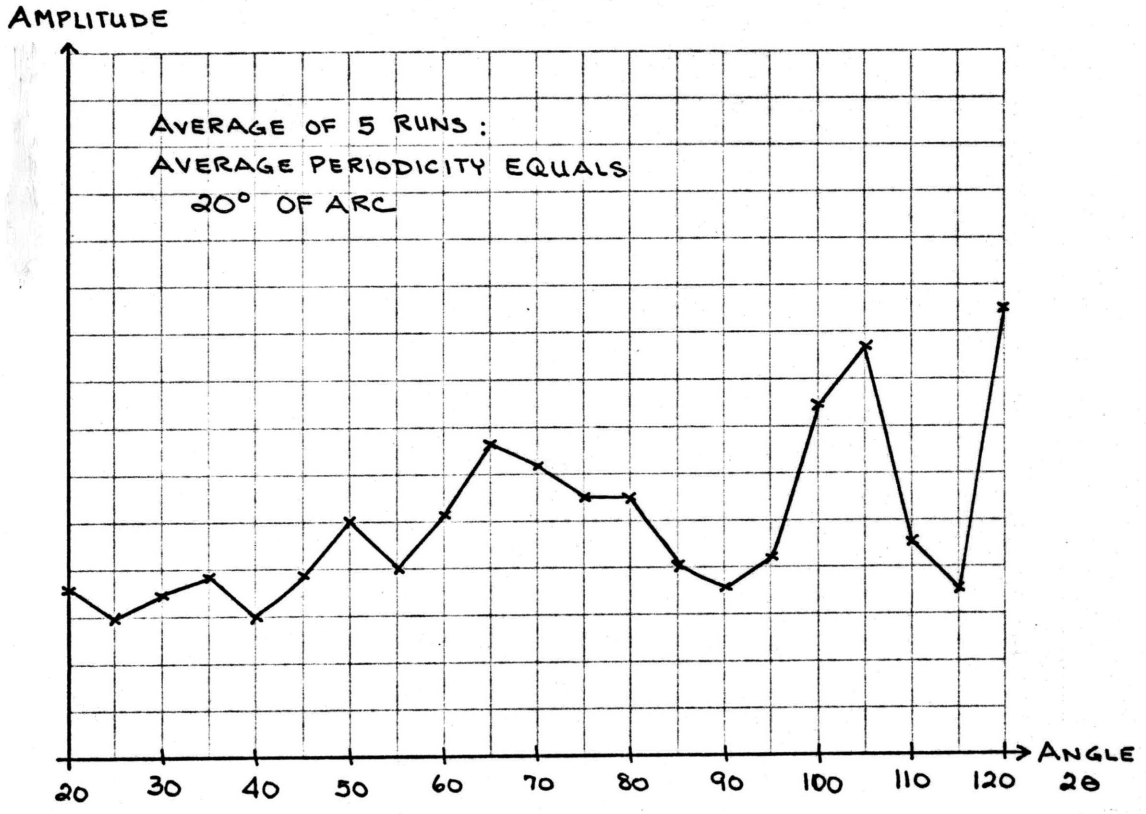

FIGURE 9: DOUBLE-ANGLE SCAN OF CALF LIVER AT 2.25 MEGAHERTZ (TRIAL 1)

Fresh calf liver in de-gassed saline.

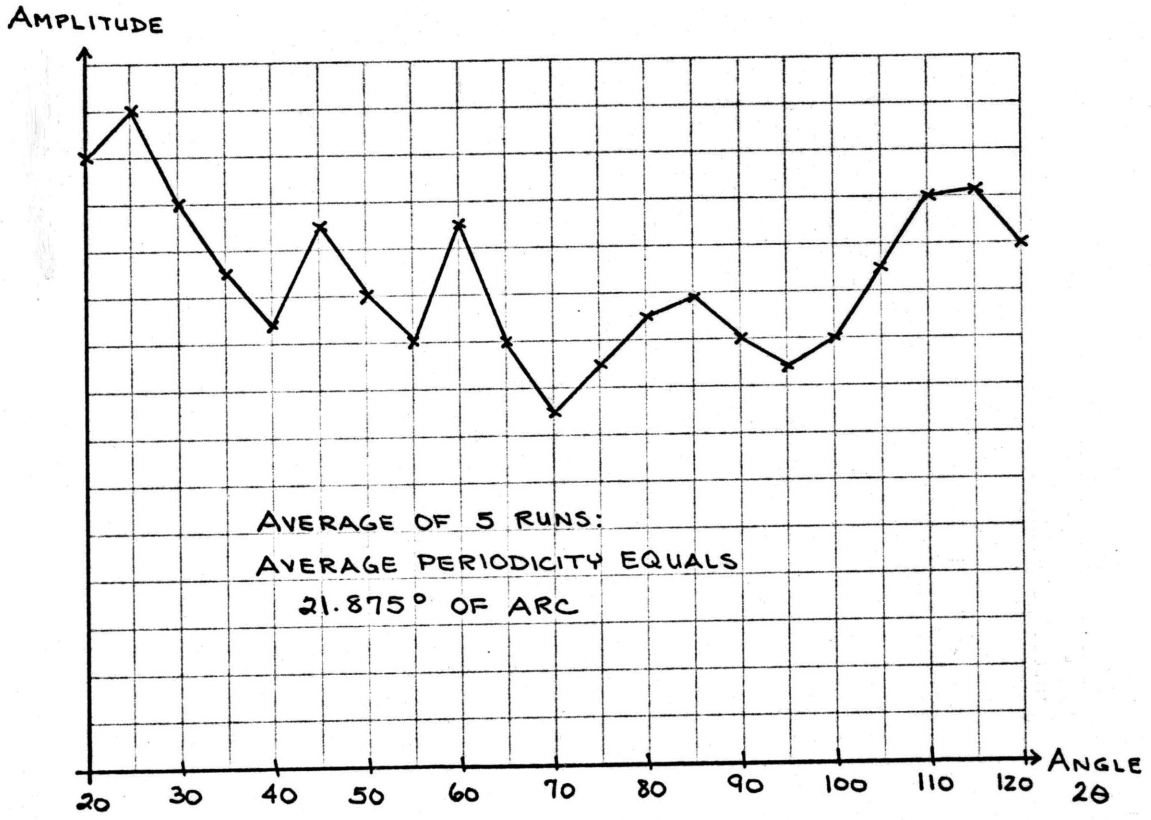

FIGURE 10: DOUBLE-ANGLE SCAN OF CALF LIVER AT 2.25 MEGAHERTZ (TRIAL2)

Fresh calf liver in de-gassed saline.

C. Frequency-Dependent Characterization of Tissue Type

Double-angle scans were performed with various tissue samples as scattering targets, and after each scattering profile was determined, and its average periodicity calculated, the ultrasonic frequency was changed, and the test repeated. Thus, we were able to correlate ultrasonic frequency with average peak separation. Orientation of the tissue appeared to effect the results very little, except in cases of marked tissue anisotropy. Again, the scatter of the data was larger than can be expected purely on the basis of the instrumentation and experimental design; the large variations appeared to be due entirely to natural variations within tissue samples from different regions of one organ, or from different animals.

The most evident trend exhibited by the frequency plots is the linearity of the relationship between angle and frequency, as shown in Figure 11, a plot of the frequency dependence of fresh calf liver in degassed saline. The best linear fit to the experimental data was determined by regression analysis, applying a least-squares curve fit. The closeness of fit can also be calculated by finding the coefficient of determination, a direct measure of accuracy of fit. For detailed discussion and formulas, see the Appendix.

Almost all the frequency-dependent plots which were made correlated very well with the least-squares line, with coefficients of determination (r^2) ranging in value from .80 to .93, all indicating excellent agreement of data and empirical line

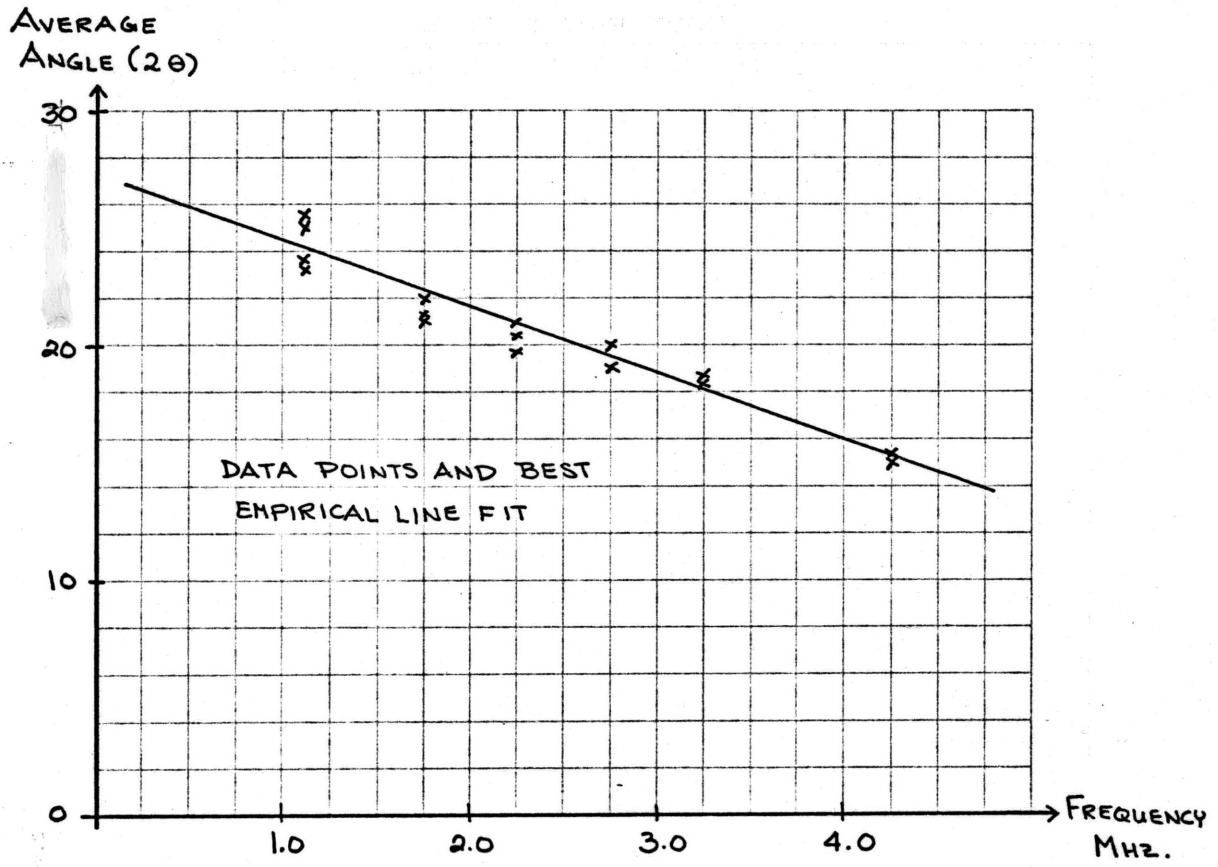

FIGURE 11: FREQUENCY DEPENDENCE OF FRESH CALF LIVER IN DE-GASSED SALINE

fit. There were some exceptions, however; certain frequency plots correlated rather poorly with a linear fit, with r^2 values in the vicinity of .50.

Frequency plots of pig liver, and calf heart muscle are shown in Figures 12 and 13, respectively. The raw data points as well as the best line fit are shown. The frequency dependences of the three tissues so far discussed were very characteristic, varying greatly in both slope and axial intercept values, and may prove to be an accurate method of cateloguing tissue scattering parameters.

D. Effect of Tissue State and Tissue Anisotropy

Calf liver tissue was used in a study of the effects of freezing and formalin fixation upon the scattering profile and the frequency dependence of biological tissues. Calf liver that had been frozen and thawed, and then examined in a series of double-angle scans at various ultrasonic transmitter frequencies, is not significantly different than the freshly excised calf liver specimens. A trend may be seen toward a general lowering of the angular values obtained, but this difference is not statistically significant at the 5% level of the t-test. This may appear to be a surprising result, since the formation of ice crystals can produce tissue structure changes; however, the only changes observed when a histological examination was made were the breakage of cell membranes, and destruction on the scale of microns. The ultrasonic scattering phenomenon measured

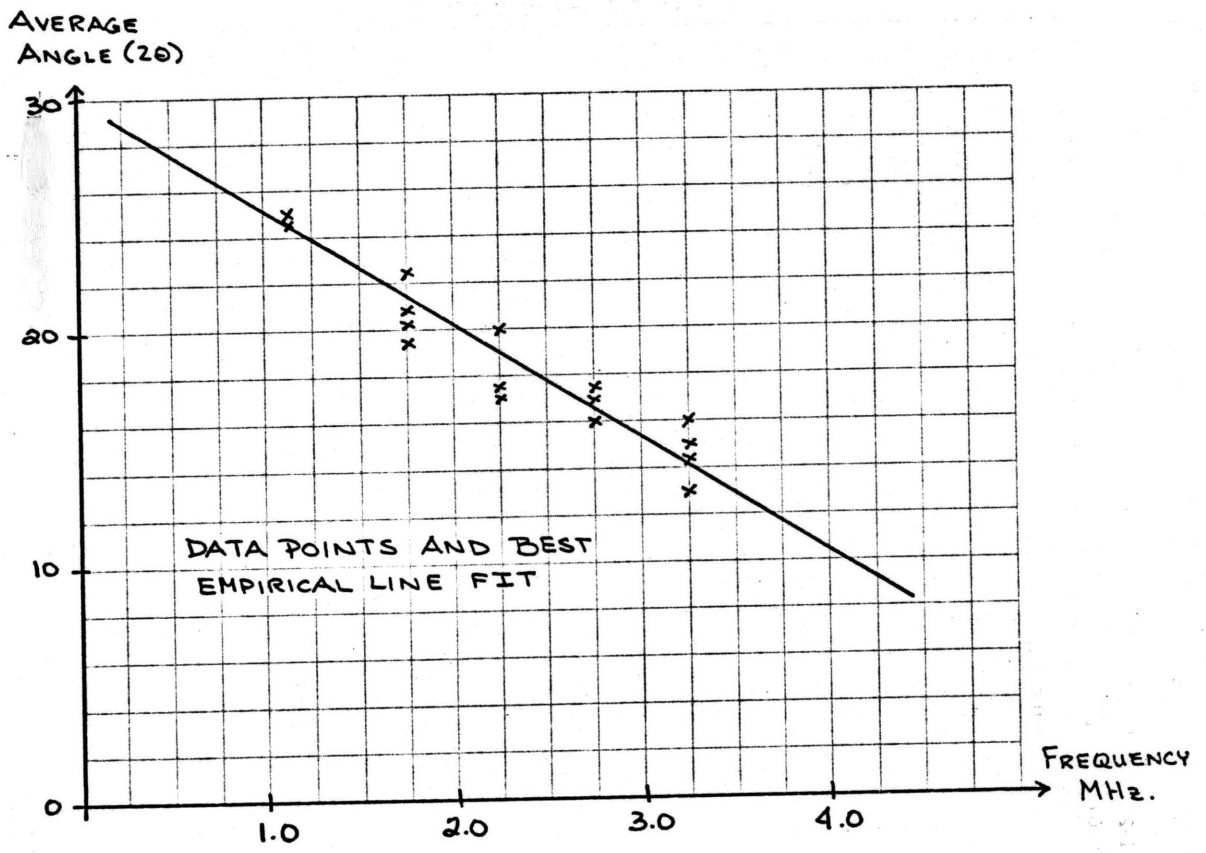

FIGURE 12: FREQUENCY DEPENDENCE OF PIG LIVER IN DE-GASSED SALINE

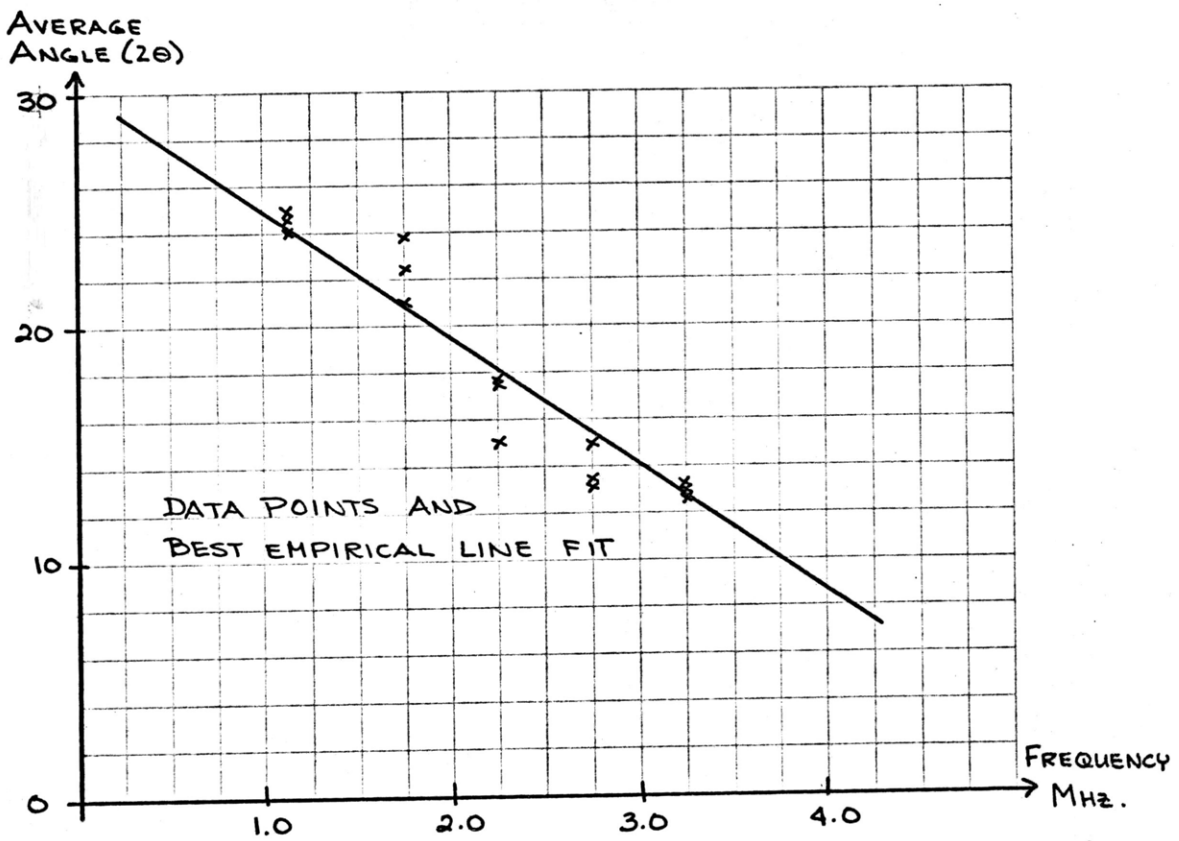

FIGURE 13: FREQUENCY DEPENDENCE OF CALF HEART MUSCLE IN DE-GASSED SALINE

in this experiment does not approach this level of resolution. The ultrasonic wavelengths used were in the sub-millimeter to millimeter range, and could not detect the damage occurring on a cellular and subcellular level.

Similar results were obtained when formalin fixed tissues were studied. Formalin fixation was not expected to change the tissue structure, but it could change the tissue elasticity, and therefore the acoustic impedence. Scattered signal strength increased in the angle-scanning of formalin-fixed tissues, but the frequency dependence change remained insignificant. Figure 14 compares the results for fresh, frozen, and formalin-fixed calf liver samples.

Certain tissues exhibit structural anisotropy which was detectable by scattering characterization. Calf skeletal muscle displays different frequency dependent behavior related to the direction at which the ultrasonic wavefront impinges upon the sample. If the cylindrical tissue plug was cut such that the muscle fiber bundles ran parallel to the cylinder height (cut "across" the grain), the resulting angular separation was higher than that of muscle cut longitudinally ("with" the grain). The differences are statistically significant, and readily recognizable, as shown in Figures 15 and 16. This structural anisotropy, and resulting dependence of scattering characteristics upon fiber orientation, was not seen in cardiac muscle samples, where no single predominant fiber orientation exists. Cutting heart

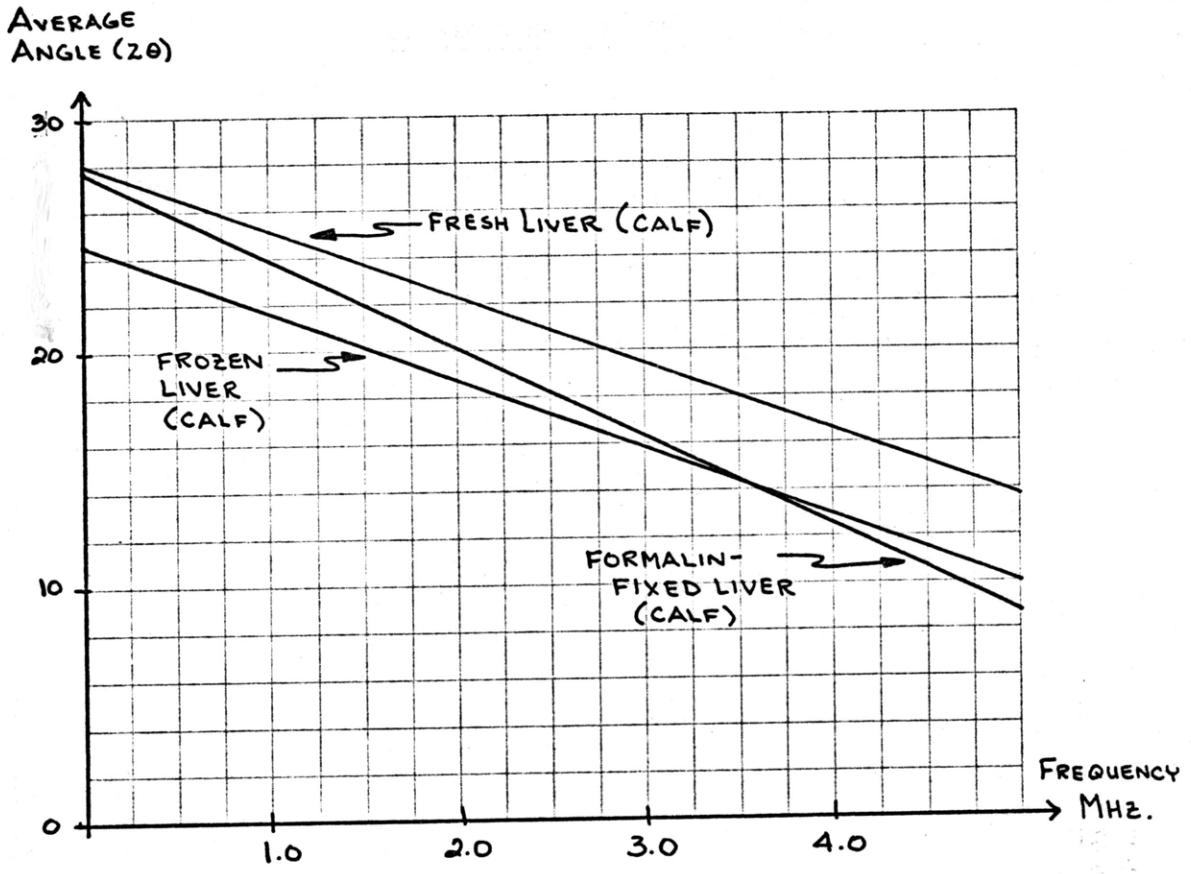

FIGURE 14: FREQUENCY DEPENDENCE COMPARISON FOR FRESH, FROZEN, AND FORMALIN-FIXED CALF LIVER

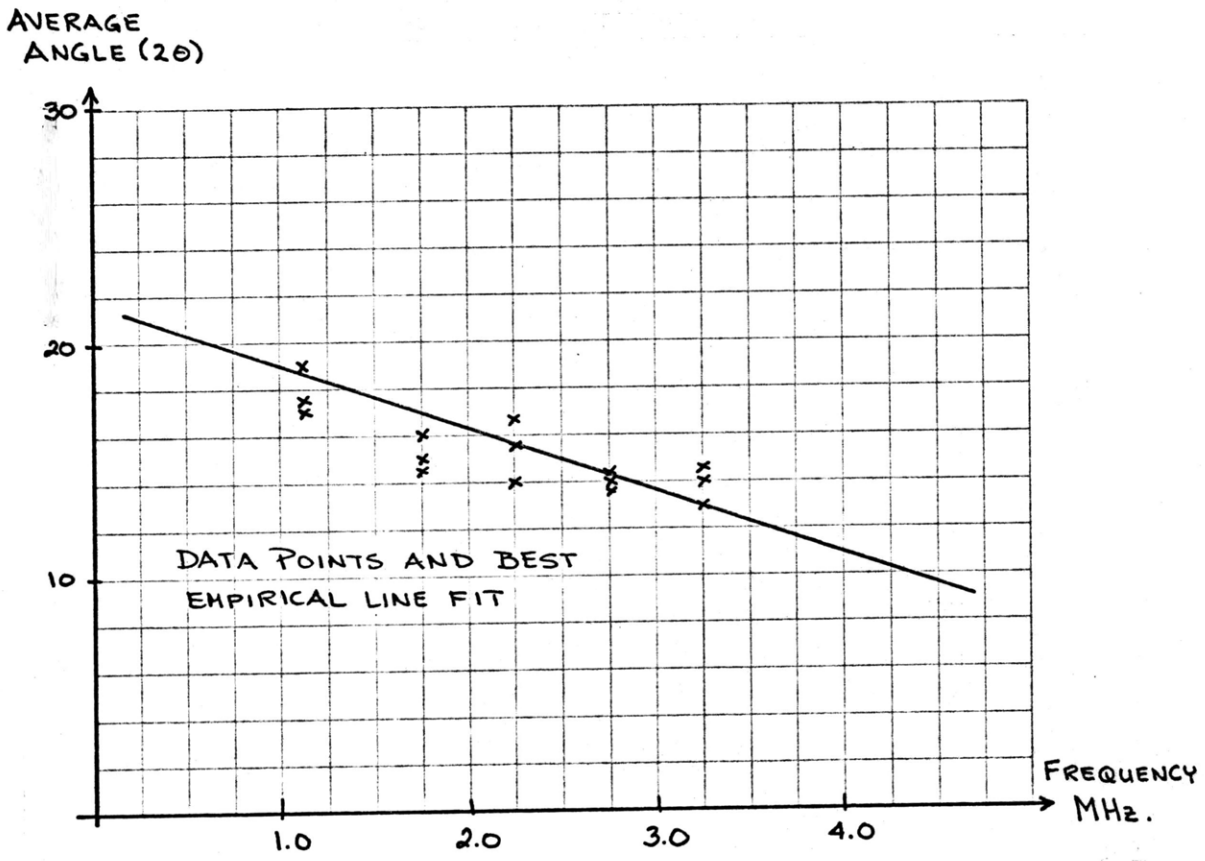

FIGURE 15: FREQUENCY DEPENDENCE OF CALF SKELETAL MUSCLE CUT ACROSS-GRAIN

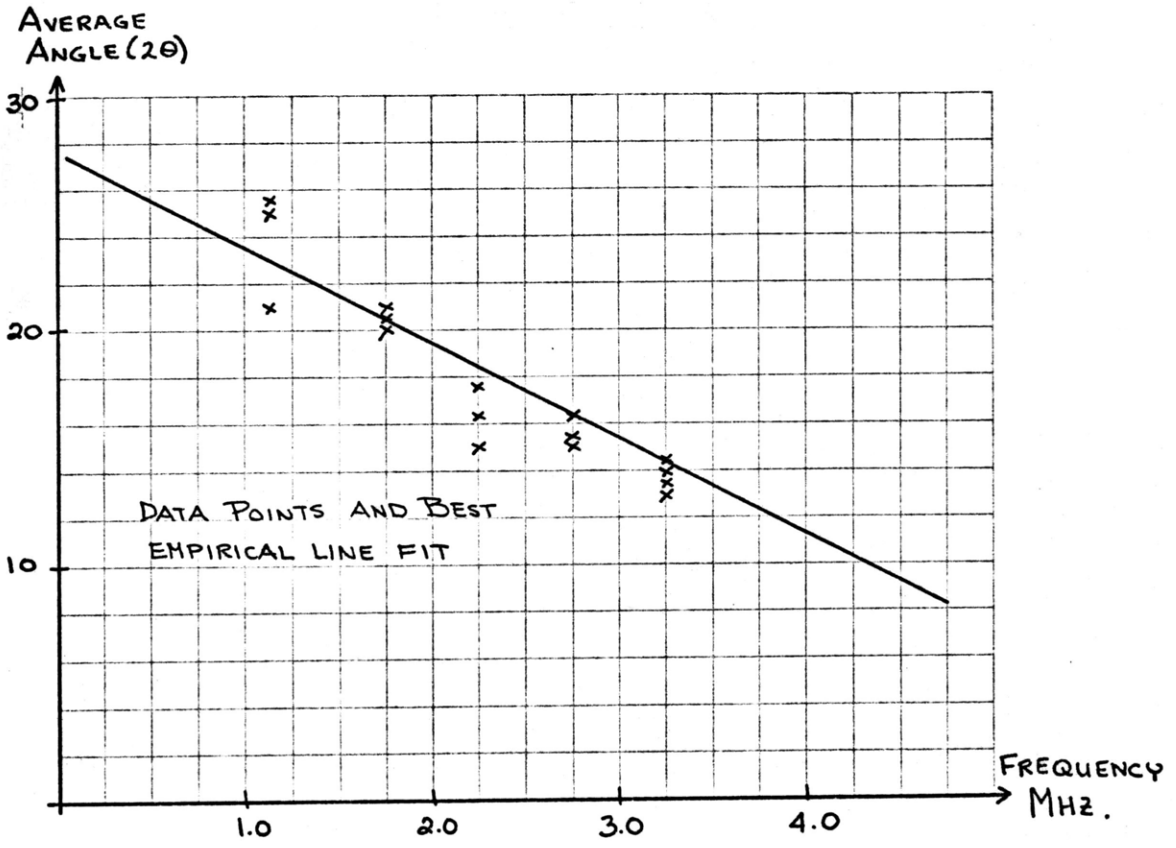

FIGURE 16: FREQUENCY DEPENDENCE OF CALF SKELETAL MUSCLE CUT LONGITUDINALLY

muscle specimens at varying planes resulted in the same frequency dependence in all cases.

CHAPTER V

DISCUSSION OF EXPERIMENTAL RESULTS

A. Statistical Comparison of Experimental Data and Bragg Differentation Theory

The experimentally-determined frequency dependence, as previously stated, appears to be linear. However, if one plots the expected dependence, predicted by Bragg's Law, the result is a hyperbolic curve. Some tissue samples appear to follow this dependence more closely than others, with calf heart muscle providing the closest correlation between experiment and theory, and calf liver being the most divergent.

To facillitate the analysis of experimental data and its correlation to Bragg theory, a second type of plot is more useful: the sine of the average periodicity angle vs. ultrasonic wavelength. On such a plot, Bragg diffraction predicts a straight line passing through the origin. By using a least squares regression, the best line of these specifications can be found. The fit is not very good, with coefficient of determination values (r^2) being less than .65 in all tissue samples under study. Thus, the phenomenon appears to be not exactly what might be expected by Bragg diffraction, yet it shows an apparent periodicity which varies with frequency in a very linear manner. The tissues under study exhibited strong differences in the frequency-dependent scattering behavior which may well be of future diagnostic use, despite the inability to directly attribute the scattering to a regular array of small reflectors, causing

interference patterns in a manner similar to x-ray crystallography.

By examining the best theoretical lines fit to the experimental data, one can calculate the best value of d, the inter-scatterer array distance, by substitution back into the Bragg condition. One can also define limits for the possible values that d can assume so to envelop the existing experimental data. Such an analysis was done for all the tissues studied, and the ranges of d values obtained are shown in Figures 17 through 21. The sine of the average angular separation is plotted vs. wavelength, and the best theoretical fit as well as the best empirical fit is demonstrated for calf liver, pig liver, calf cardiac muscle, and calf skeletal muscle.

The possible reasons for the discrepancy between Bragg theory and experimental observations are many. The most probable explanation is the notion that biological tissue samples may not be ordered in an array which is regular enough at the sub-millimeter to millimeter scale. Observation of histological slides of the tissues investigated tends to confirm this. There exists a great deal of order on a smaller scale, and order is apparent even at the scale which is resolved by the ultrasonic scattering measurement apparatus; however, the regularity with which the clusters of ordered elements are arranged is very slight. For example, muscle fibers are very well ordered, all have the same orientation, and they are grouped together into bundles surrounded by sheaths of connective tissue. These bundles of fibers are

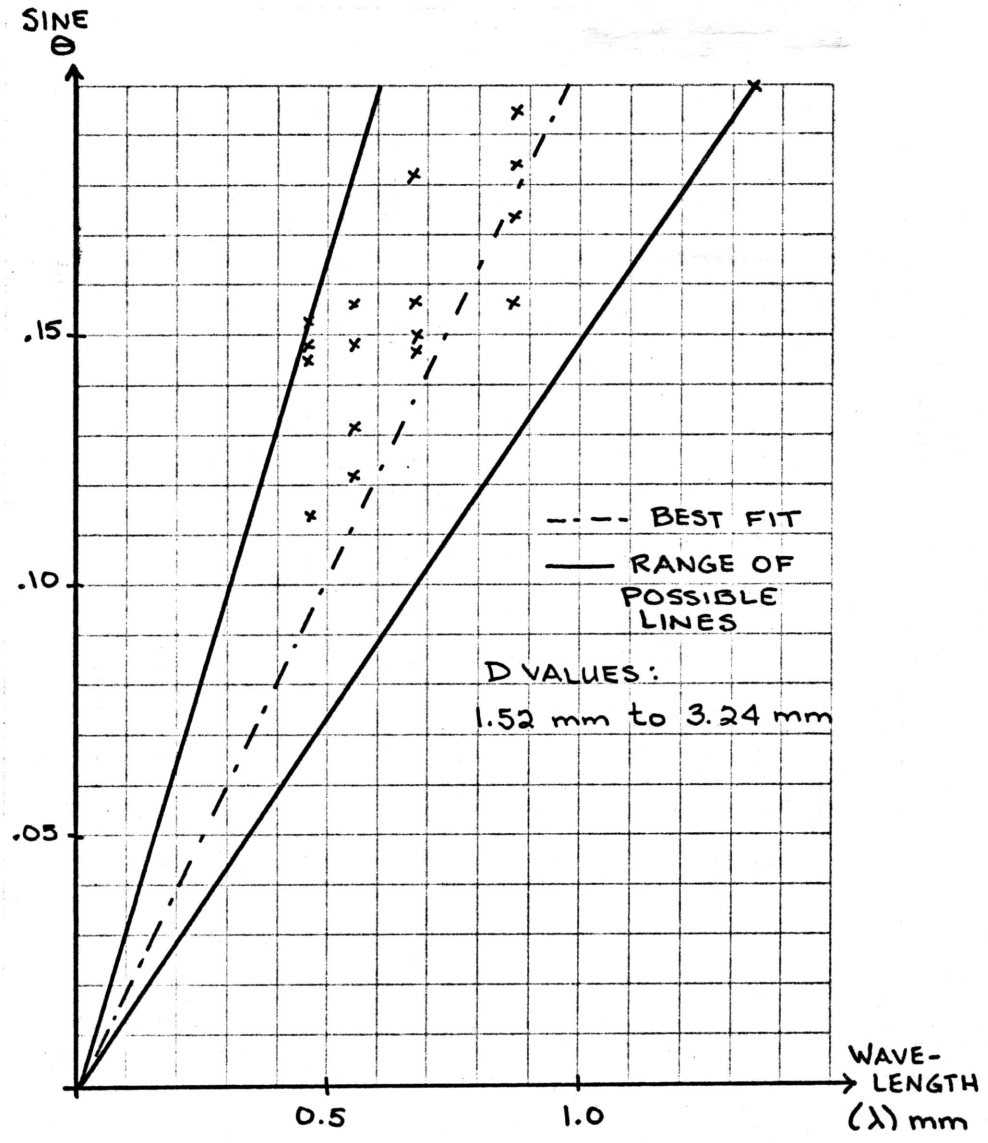

FIGURE 17: COMPARISON OF THEORY AND EXPERIMENTAL RESULTS - CALF LIVER

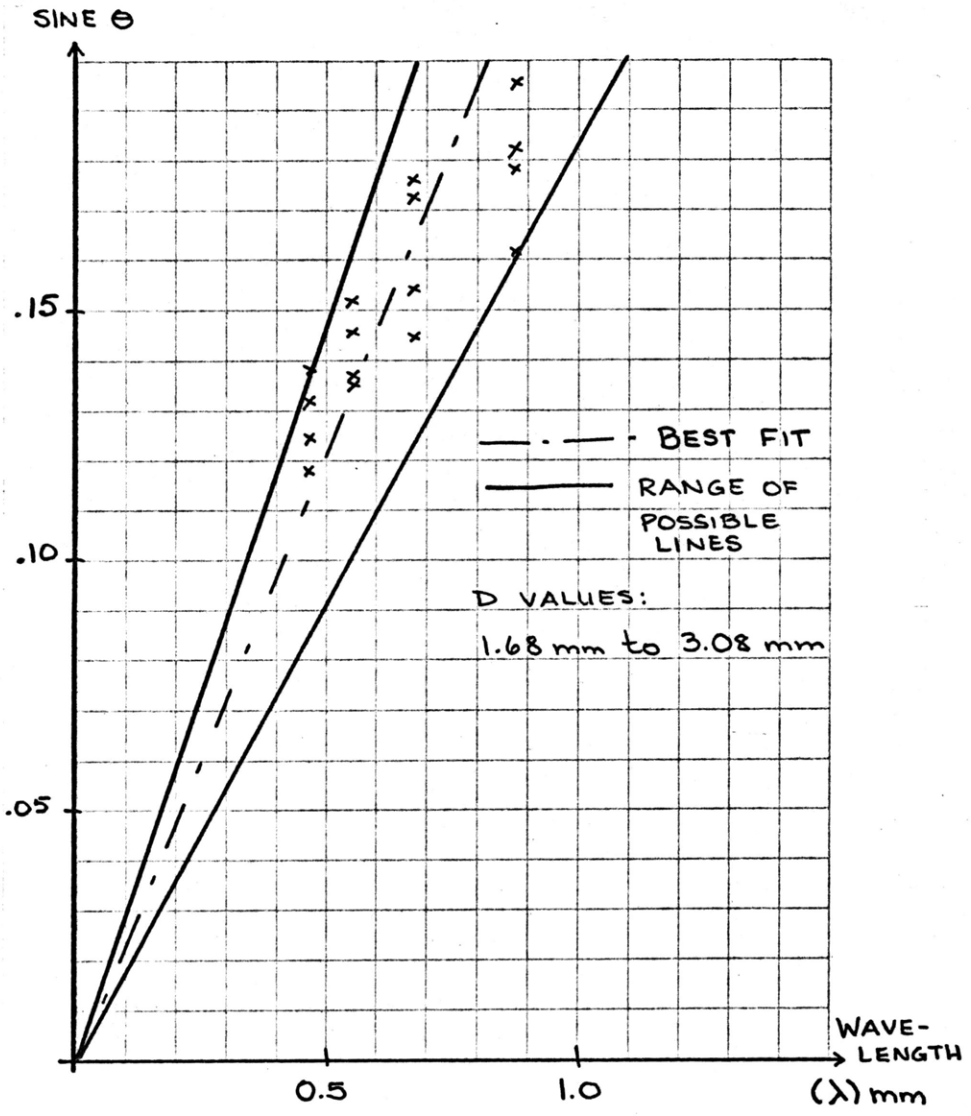

FIGURE 18: COMPARISON OF THEORY AND EXPERIMENTAL RESULTS - PIG LIVER

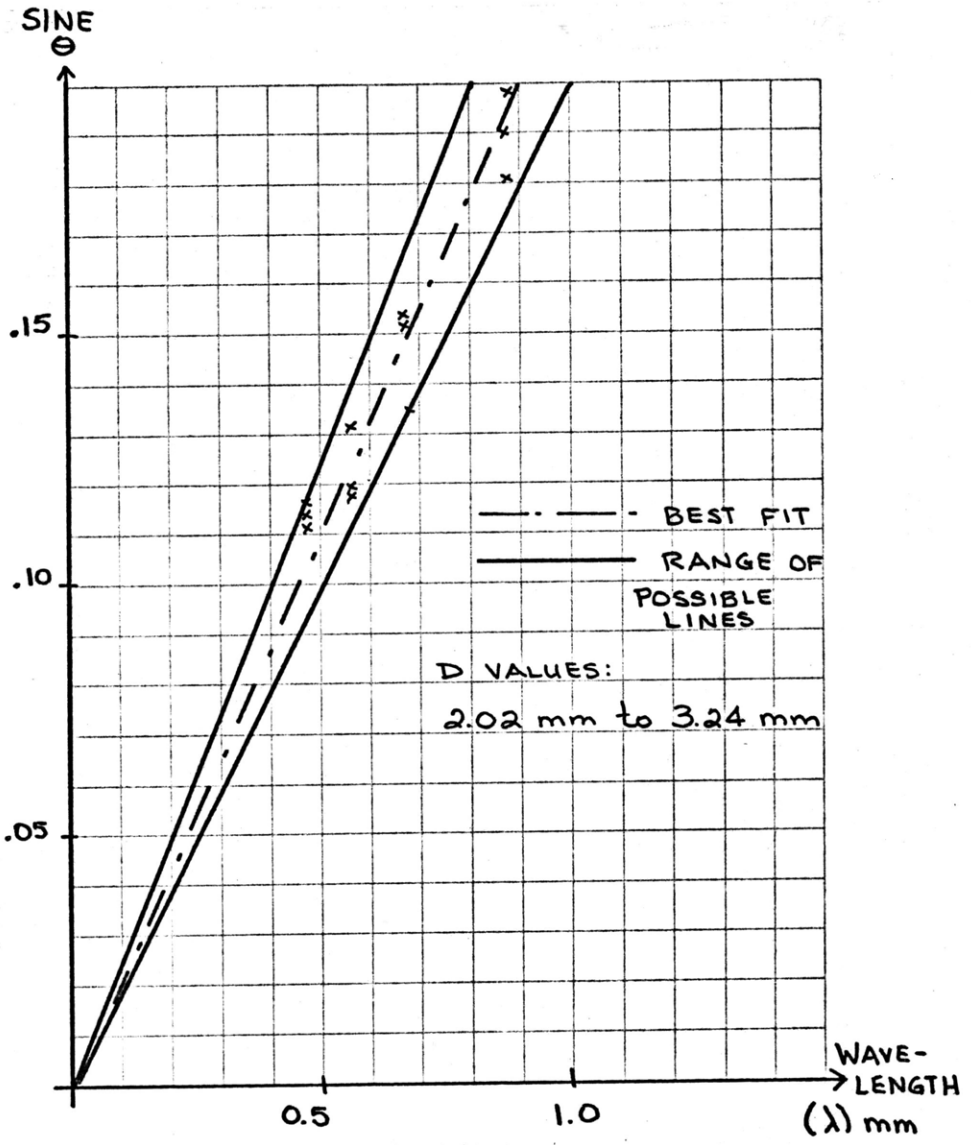

FIGURE 19: COMPARISON OF THEORY AND EXPERIMENTAL RESULTS - CALF CARDIAC MUSCLE

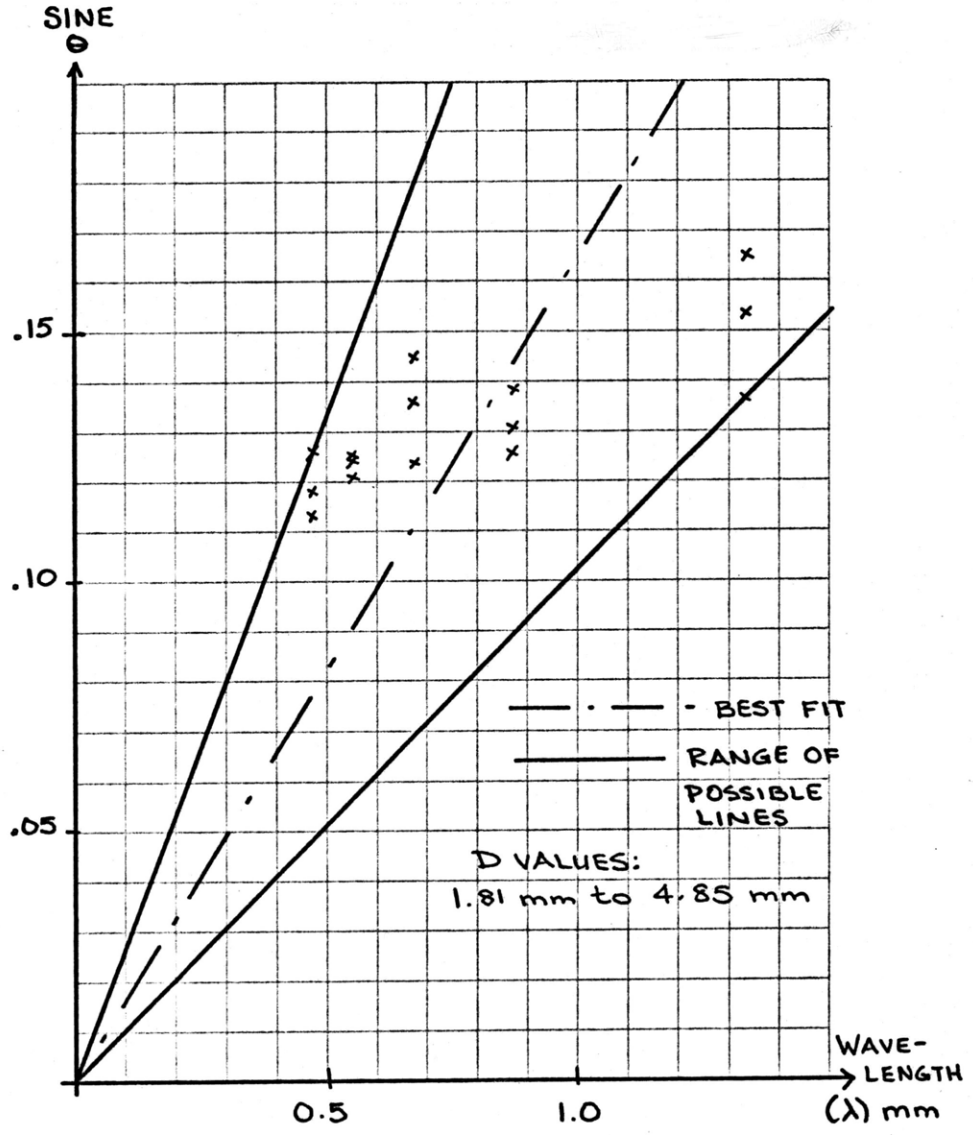

FIGURE 20: COMPARISON OF THEORY AND EXPERIMENTAL RESULTS - CALF SKELETAL MUSCLE CUT ACROSS-GRAIN

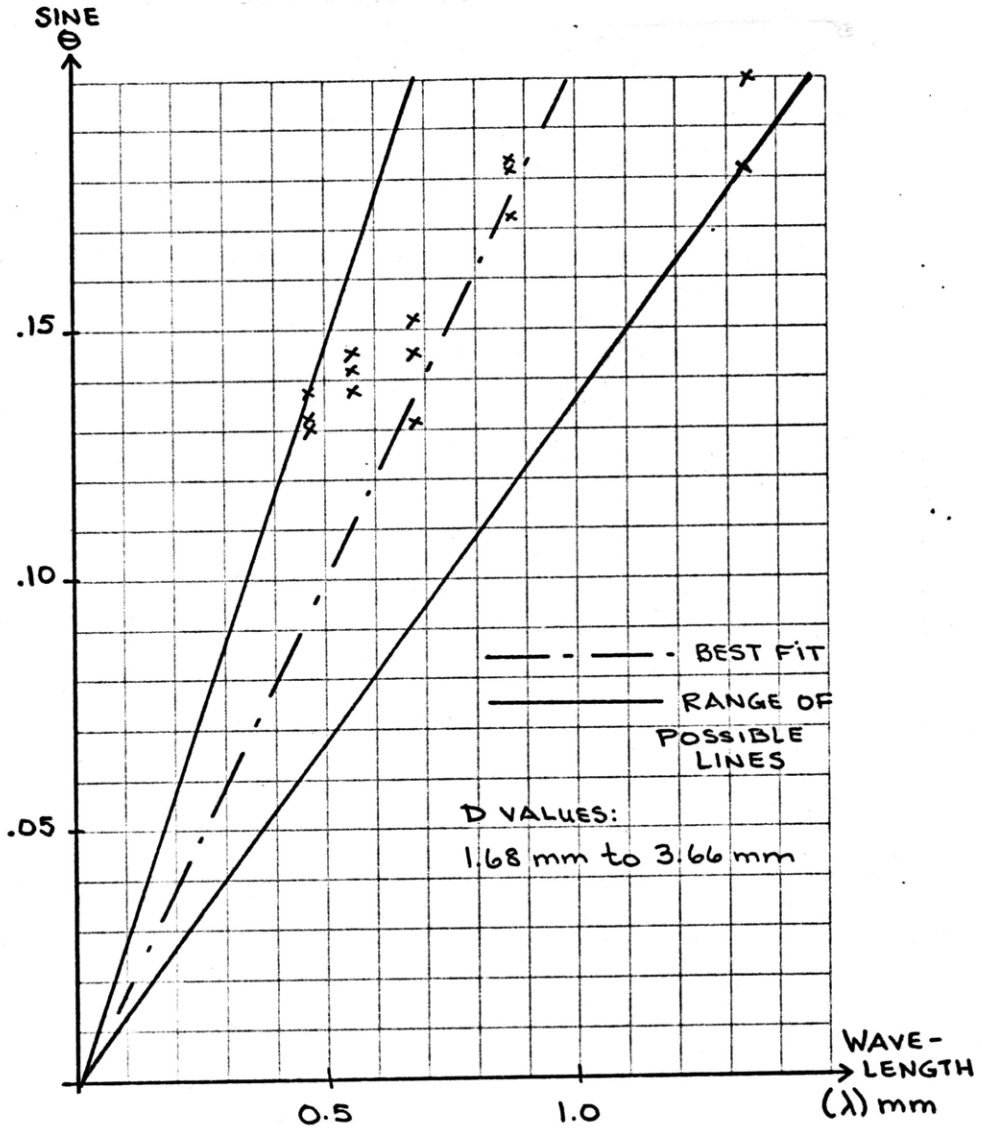

FIGURE 21: COMPARISON OF THEORY AND EXPERIMENTAL RESULTS - CALF SKELETAL MUSCLE CUT LONGITUDINALLY

not very consistent in diameter, and the ordered array which is seen is composed of bundles of many varying diameters. It seems possible that enough regularity exists to give rise to the periodicity evidenced in the ultrasonic internal scattering profiles, but perhaps not enough strict matrix ordering is present to give the full manifestations of Bragg diffraction phenomena.

B. Diagnostic Implications of the Scattering Data

Despite the apparent disagreement between the results seen and the predicted values for Bragg diffraction, the internal scattering properties of biological tissues hold the promise of being significant for diagnostic applications. Tissues which have structural differences that occur within the resolving power of the ultrasound (limited by the size of the wavelength) are easily distinguished by means of their characteristic frequency-dependent scattering. For example, calf and pig liver are structurally different in their organization of cells into clusters. Pig liver, even with the unaided eye, appears to have a honeycombed, hexagonal organizational unit, which is probably the theorized scattering element. These clusters, like the muscle fiber bundles, appear to vary in diameter. Calf liver has far less obvious a unit of structural regularity. The cell clusters are present, but not as well defined in shape as are those of pig liver. It is interesting to note that the most regular and organized of the tissue samples, cardiac muscle, also exhibited the closest correlation to the ideal Bragg theory.

The muscle fiber bundles were very regular in diameter despite the lack of one predominant orientation direction. Another factor that may lead to the non-ideal results is the irregularity introduced into the array by the presence of blood vessels dispersed through out the tissue, leading to discontinuities in the array structure.

Work with tissue specimens of known pathology is necessary to determine more precisely the diagnostic utility of scattering characterizations. An interesting extension of this experiment might involve the scattering changes which occur in cirrhotic liver and in fatty necrosis, both of which disrupt the structure by introducing fat globules and many randomly-oriented fibers. Such pathologies can be induced in experimental animals by the feeding of certain toxic substances, such as alcohol or CCl_4, to overload the liver's de-toxification apparatus. A study of the disease's progression with time can then be correlated to the changes in ultrasonic scattering properties.

The frequency-dependent phenomena exhibited by various tissues seem to be the best method of characterizing tissue type: better than looking at either the double-angle scan alone, or than studying the surface scattering properties. However, diagnostically, frequency-dependence behavior would be cumbersome and time-consuming to measure. A better technique is needed to implement the same principle for <u>in vivo</u> diagnostic use. A better method might be to keep the transducers at a fixed angle, and to do a continuous sweep of frequency to measure the

amplitude vs. frequency profile. A scan such as this should take less time, and could be performed using existing B-scan diagnostic equipment with minor modifications.

It is still too early to assess the possible impact of internal scattering measurements as a new diagnostic tool. Certain limitations are already apparent: resolution and accessibility. As previously discussed, the resolving power is limited by the ultrasonic wavelength. Use of higher frequencies would produce a system with increased tissue resolution; however, at higher frequencies tissue absorption becomes a problem, and less energy input is required to heat the tissue, as well as the related technical problem of a decreased signal strength to be measured. There are, as a result, certain pathologies which may never be detectable by this method. Only structural changes of a fairly gross nature are measureable.

The problem of accessibility of the organ or tissue under study is also important. For the diagnostic technique to be safe and non-invasive, the measurements must be made at the skin, through all the intervening tissues and organs in the path of the ultrasonic beam. The use of a time-gated mechanism can localize the region of interest; however, attenuation and loss of signal strength is again a problem. This is especially true if there are significant acoustic impedence mismatch barriers, such as bones or the lungs, intervening between the skin and the target area.

CHAPTER VI

CONCLUSION

Diagnostic ultrasonics may soon have access to a new method of characterizing tissues on the basis of their interactions with an ultrasonic field. Internal scattering properties of tissues can provide structural information correlated to possible pathology, and can be measured accurately and in a non-invasive manner.

Preliminary work has shown that the scattering phenomenon occurring may be related to Bragg diffraction, but is probably not completely analogous, due to the tissue inhomogeneity and the great biological variability possible. Tissues are not ideal arrays, but do show considerable regularity which can account for their scattering periodicity.

In summary, biological tissues can be characterized on the basis of their frequency-dependent internal scattering behavior, and some correlations can be made with the exact tissue structure by analysis of the experimental results and their comparison to ideal Bragg diffraction phenomena. Further study is necessary to design an optimal system for diagnostic use; limitations must be realistically assessed, and tissue pathologies must be catelogued on the basis of the changes which are manifest in their internal scattering behavior.

BIBLIOGRAPHY

1. Wells, P. N. T., Physical Principles of Ultrasonic Diagnosis, Academic Press, New York, 1969.
2. Dunn, F., Edmonds, P. D., Fry, W. J., "Absorption and Dispersion of Ultrasound in Biological Media," Biological Engineering, H. P. Schwan, ed., 1969.
3. Namery, J., "Ultrasonic Detection of Myocardial Infarction in Dog," M.I.T. Department of Electrical Engineering, M.S. Thesis, June 1973.
4. Senapati, N., Lele, P. P., Woodin, A., "A Study of the Scattering of Sub-Millimeter Ultrasound from Tissues and Organs," Proceedings of 1972 Ultrasonics Symposium, Boston, IEEE.
5. Knoft, L., "Frequency Dependence of Scattered Elastic Waves," J. Acous. Soc. Amer., 42, 1967.
6. Wells, P. N. T., op. cit.
7. Waag, R. C., Lerner, R. M., "Tissue Macrostructure Determination with Swept-Frequency Ultrasound," Proceedings of 1973 Ultrasonic Symposium, Monterey, IEEE.
8. Azaroff, L. V., Elements of X-Ray Crystallography, McGraw-Hill, New York, 1968.
9. Gurnier, A., X-Ray Diffraction, W. H. Freeman and Company, San Francisco, 1963.
10. Senapati, N., Lele, P. P., Woodin, A., op. cit.

11. Mountford, R., Wells, P. N. T., "Ultrasonic Liver Scanning: The A-Scan in the Normal and Cirrhosis," Phys. in Med. Biol., 17, 1972.

12. Freese, M., Makow, D., "Ultrasound Backscatter in Fresh and Thawed Animal Tissue," J. Fish. Res. Bd. Canada, 25, 1968.

13. Hill, C. R., Chivers, R. C., "Investigations of Backscattering in Relation to Ultrasonic Diagnosis," Conference Proceedings UBIOMED 70, Warsaw, 1970.

14. Chivers, R. C., Hill, C. R., Nicholas, D., "Frequency Dependence of Ultrasonic Back-Scattering Cross-Sections: An Indicator of Tissue Structure Characteristics," Ultra-Sonics in Medicine, M. de Vlieger, D. N. White, V. R. McCready, editors, Excerpta Medica, 1973.

15. Hill, C. R., "Interactions of Ultrasound with Tissues, Ultrasonics in Medicine, M. de Vlieger, D. N. White, V. R. McCready, editors, Excerpta Medica, 1973.

16. Chivers, R. C., Hill, C. R., "A Spectral Approach to Ultra-Sonic Scattering from Human Tissue: Methods, Objectives, and Backscattering Measurements," Phys. Med. Biol., 20, 1975.

17. Waag, R. C., Gramiak, R., Lerner, R. H., "Ultrasonic Determination of Cardiac Macrostructure," Cardiac Ultra-Sound, R. Gramiak, R. C. Waag, editors, C. V. Mosby, St. Louis, 1975.

18. Hill, C. R., op. cit.

19. Waag, R. C., Gramiak, R., Lerner, R. H., op. cit.

20. Wells, P. N. T., op. cit.

21. Ibid.

22. Laboratory Techniques Manual, M.I.T. Department of Chemistry, Vol. I, 1974.

APPENDIX

LEAST SQUARES CURVE FIT

Least-Squares Curve Fit

Linear fit: $y = mx + b$

Regression coefficients:

$$m = \text{slope} = \frac{N\Sigma x_i y_i - \Sigma x_i \Sigma y_i}{N\Sigma x_i^2 - (\Sigma x_i)^2}$$

$$b = \text{intercept} = \frac{\Sigma y_i - m\Sigma x_i}{N}$$

where: N = number of observations

x = independent variable

y = dependent variable.

Coefficient of Determination:

$$r^2 = \frac{[\Sigma x_i y_i - \frac{\Sigma x_i y_i}{N}]^2}{[\Sigma x_i^2 - \frac{(\Sigma x_i)^2}{N}][\Sigma y_i^2 - \frac{(\Sigma y_i^2)}{N}]}$$

$0 < r^2 < 1$

$r^2 = 1$ for perfect fit

(Source: Draper, N. R., Smith, H., Applied Regression Analysis, John Wiley, New York, 1968.)